ANALYSIS OF HEAT TRANSFER IN DUCT FLOW WITH WALL ENERGY STORAGE

L. D. L. Montenegro, luizmontenegro@mec.uff.br
L. A. Sphaier, lasphaier@mec.uff.br
Laboratório de Mecânica Teórica e Aplicada, Programa de Pós-Graduação em Engenharia Mecânica, Departamento de Engenharia Mecânica, Universidade Federal Fluminense, Rua Passo da Pátria 156, bloco E, sala 216, Niterói, RJ, 24210-240, Brazil

Abstract. *In a moment that the world seeks sustainable development, many of the aggressions that the planet has been suffering since long become dormant today. The hole in the ozone layer and global warming are evidence of that. Engineers have always dealt with thermal machines assuming that the temperature of the thermal reservoir in which heat was despised as constant. Due to this hypothesis assumed that we observe the planet's temperature is rising every year. In this scenario the search for sustainable development, ie development which does not undermine the ability of nature to recover from damage caused by man, the regenerator heat becomes even more important. The characteristics of the regenerator heat are extremely favorable in the quest for sustainable development, since its function is to increase the efficiency of heat engine pre-heating the working fluid before the heating process itself by making an energy that would be thrown out at first. In this paper the Nusselt number is calculated for the problem of flow between parallel plates kinetically developed and developing heat using the finite volume method with a UDS (upwind difference scheme) approximation of advective terms and with non-uniform mesh, so we can describe the behavior of the number Nusselt microchannels in the regenerators.*

Keywords: *heat exchanger, regenerator, computational simulation*

1. INTRODUCTION

There are uncountable processes which require heat transfer between different process streams. As a result, heat exchanging devices have numerous applications in practically all kinds of industry. Whenever size is a problem, compact heat exchangers are necessary. One class of exchangers that serve for that purpose is that of heat regenerators. These type of exchangers rely on indirect heat transfer with a solid carrier (the regenerator matrix) serving as the means to convey heat from one process stream to the other. As a result, the operation of these types of exchangers is periodic, also termed a quasi-steady regime. In this regime, a repetitive transient solution occur in each cycle. Due to the cyclic nature of this problem, the behavior of the convective heat transfer coefficient can be quite different than that found in steady state operation. Nevertheless, apparently all formulations for heat regenerators (Holmberg, 1977; Shen and Worek, 1992, 1993b,a; de Monte, 1999; Saastamoinen, 1999; Sphaier and Worek, 2004, 2009), including those for sensible and latent heat regenerators, are based on considering constant convective transfer coefficients – which occurs for steady thermally developed flow with either constant temperature or constant heat flux at the wall. This paper aims to investigate the effects of transient heat transfer in a mini duct with laminar flow that has application in regenerative heat exchangers. The objective os this study is to analyze the variation of convective heat transfer coefficient in transient heat transfer with energy storage in the channel wall, simulating conditions found in regenerative heat exchangers. The behavior of the Nusselt number for heat transfer in thermally developing flow using a non-uniform and mesh with further refinement in the entrance region due to the difficulty of calculating the Nusselt number at that location. Numerical simulations of the problem considering parallel plates channels are carried out using the Finite Volumes Method with the UDS (upwind difference scheme is a method that takes into account the direction of flow, therefore can only be applied to advective terms) and CDS (central difference scheme is a method that does not take into account the flow direction, can be used for advective and diffusive terms). The data resulting from this investigation will allow one to determine the correct behavior for the Nusselt number.

Figure 1 shows the schematic of a regenerative heat exchanger.

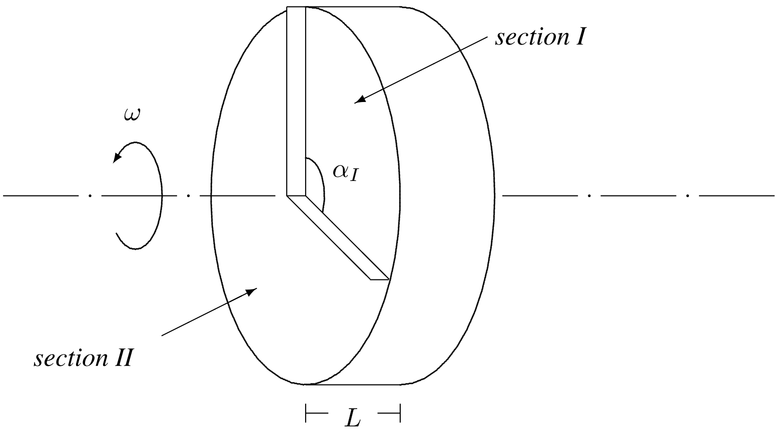

Figure 1. Rotary regenerator.

The following nomenclature was used:

U	Dimensionless velocity
$\bar{u}$	Average speed
ξ	dimensionless length
η	dimensionless length
τ	dimensionless time
Dimensionless groups	
Pe	Péclet number
Nu	Nusselt number
Fo	Fourier number
Fo_s	Fourier number for solid wall
R^*	Resistance rate
Subscripts	
P	Center
N	North
S	South
E	East
W	West
SW	South-west
SE	South-east
SS	South of the south volume
w	West node
sw	South-west node

2. PROBLEM FORMULATION

Figure 2 represents the flow in mini channels in the matrix of the rotary regenerator.

The formulation for this problem is based on the the following governing equation:

$$\mathrm{Fo}^{-1}\frac{\partial\theta}{\partial\tau} + \frac{1}{2}U\frac{\partial\theta}{\partial\xi} = \mathrm{Pe}_H^{-2}\frac{\partial^2\theta}{\partial\xi^2} + \frac{\partial^2\theta}{\partial\eta^2}, \tag{1}$$

where the dimensionless quantities are given by:

$$\theta = \frac{T - T_{\min}}{T_{\max} - T_{\min}}, \qquad \eta = \frac{y}{H/2}, \qquad \xi = \frac{x}{L}, \tag{2}$$

and the value of L is chosen from a scale analysis of the thermal entry length:

$$L \sim \frac{H}{2}\,\mathrm{Pe}_H, \qquad \text{with} \qquad \mathrm{Pe}_H = \frac{\bar{u}\,H}{\alpha}. \tag{3}$$

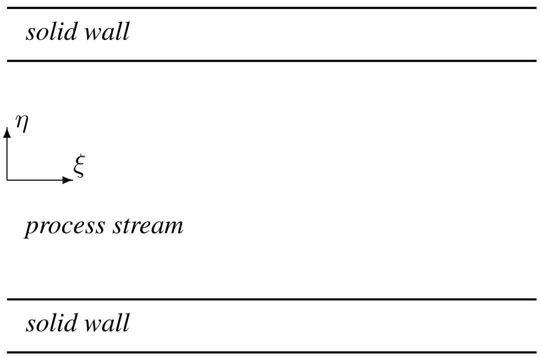

Figure 2. scheme of the flow in the channel.

Equation (1) is simplified for large Pe_H, as found in gas flows in heat regenerators, leading to:

$$\mathrm{Fo}^{-1}\,\frac{\partial\theta}{\partial\tau} + \frac{1}{2}\,U\,\frac{\partial\theta}{\partial\xi} = \frac{\partial^2\theta}{\partial\eta^2}, \tag{4}$$

The boundary conditions for this problem (considering a balanced cross-flow exchanger) are given by:

$$R^*\,\frac{\partial\theta}{\partial\eta} = -\mathrm{Fo}_s^{-1}\,\frac{\partial\theta}{\partial\tau} \qquad \text{for} \qquad \eta = 1, \qquad\qquad \left(\frac{\partial\theta}{\partial\eta}\right)_{\eta=0} = 0, \tag{5}$$

$$\theta(0,\eta) = 1 \qquad \text{for} \qquad 0 \le \tau < 1/2 \tag{6}$$

$$\theta(\xi_f,\eta) = 0 \qquad \text{for} \qquad 1/2 \le \tau < 1 \tag{7}$$

$$\theta(\xi,\eta,0) = 0. \tag{8}$$

Where the Fourier number is defined in terms of thickness of the main direction of heat conduction (H/2), the final time t_f and thermal diffusivity of the fluid α.

$$\mathrm{Fo} = \frac{\alpha\,t_f}{(H/2)^2}, \tag{9}$$

Fourier number for solid wall, which is similar to the fluid, but the thickness and thermal diffusivity are considered solid, and the ratio of the thermal resistances of conduction in the transverse direction is defined as:

$$\mathrm{Fo}_s = \frac{\alpha_s\,t_f}{(\delta/2)^2}, \tag{10}$$

Resistance rate:

$$R^* = \frac{k\,(\delta/2)}{k_s\,(H/2)} \tag{11}$$

The dimensionless velocity is given by the Hagen-Poiseuille profile:

$$U = \frac{u}{\bar{u}} = \frac{3}{2}\,(1-\eta^2). \tag{12}$$

However, if a simplified slug-flow case is considered, $U = 1$ and the previous equations are modified.

The Nusselt number is calculated from:

$$\mathrm{Nu}_{D_H} = \frac{-4\,(\partial\theta/\partial\eta)_{\eta=1}}{\int_0^1 U\theta\,\mathrm{d}\eta}. \tag{13}$$

A preliminary implementation (based on a combination of the Finite Volumes Method and the Numerical Method of Lines) for calculating the Nusselt number in transient flow with constant wall temperature was performed in previous studies (Nogueira and Sphaier, 2009, 2008). This study greatly extends this implementation, providing a means of calculating the Nusselt number in a situation that resembles the real operation of heat regenerators.

3. NUMERICAL SOLUTION

Non-uniform grid in the axial direction is employed and integration leads to:

$$\mathrm{Fo}^{-1}\int_{\eta_s}^{\eta_n}\int_{\xi_w}^{\xi_e}\frac{\partial\theta}{\partial\tau}\,\mathrm{d}\xi\,\mathrm{d}\eta+\frac{1}{2}\int_{\eta_s}^{\eta_n}\int_{\xi_w}^{\xi_e}\frac{\partial}{\partial\xi}(U\,\theta)\,\mathrm{d}\xi\,\mathrm{d}\eta=\int_{\eta_s}^{\eta_n}\int_{\xi_w}^{\xi_e}\frac{\partial^2\theta}{\partial\eta^2}\,\mathrm{d}\xi\,\mathrm{d}\eta, \tag{14}$$

$$\mathrm{Fo}^{-1}\int_{\eta_s}^{\eta_n}\int_{\xi_w}^{\xi_e}\frac{\partial\theta}{\partial\tau}\,\mathrm{d}\xi\,\mathrm{d}\eta+\frac{1}{2}\int_{\eta_s}^{\eta_n}U\,(\theta)\big|_{\xi_w}^{\xi_e}\,\mathrm{d}\eta=\int_{\xi_w}^{\xi_e}\left(\frac{\partial\theta}{\partial\eta}\right)\bigg|_{\eta_s}^{\eta_n}\mathrm{d}\xi, \tag{15}$$

The grid is non-uniform in ξ with computational nodes centered between cell faces. As a result, the following integral approximations apply:

$$\int_{\eta_s}^{\eta_n}\int_{\xi_w}^{\xi_e}\frac{\partial\theta}{\partial\tau}\,\mathrm{d}\eta\,\mathrm{d}\xi\approx\frac{\mathrm{d}\theta_P}{\mathrm{d}\tau}\Delta\xi_P\,\Delta\eta \tag{16}$$

$$\int_{\eta_s}^{\eta_n}U\,(\theta)\big|_{\xi_w}^{\xi_e}\,\mathrm{d}\eta\approx U_P\,(\theta_e-\theta_w)\,\Delta\eta \tag{17}$$

$$\int_{\xi_w}^{\xi_e}\left(\frac{\partial\theta}{\partial\eta}\right)\bigg|_{\eta_s}^{\eta_n}\mathrm{d}\xi\approx\left[\left(\frac{\partial\theta}{\partial\eta}\right)_n-\left(\frac{\partial\theta}{\partial\eta}\right)_s\right]\Delta\xi_P \tag{18}$$

Approximated equation:

$$\mathrm{Fo}^{-1}\frac{\mathrm{d}\theta_P}{\mathrm{d}\tau}+\frac{1}{2}U_P\,\frac{\theta_e-\theta_w}{\Delta\xi_P}=\frac{1}{\Delta\eta}\left[\left(\frac{\partial\theta}{\partial\eta}\right)_n-\left(\frac{\partial\theta}{\partial\eta}\right)_s\right] \tag{19}$$

Interpolation rules:

$$\left(\frac{\partial\theta}{\partial\eta}\right)_n\approx\frac{\theta_N-\theta_P}{\Delta\eta},\qquad\left(\frac{\partial\theta}{\partial\eta}\right)_s\approx\frac{\theta_P-\theta_S}{\Delta\eta} \tag{20}$$

CDS approximation for advection term:

$$\theta_e\approx\frac{\theta_P\,\Delta\xi_E+\theta_E\,\Delta\xi_P}{\Delta\xi_P+\Delta\xi_E},\qquad\theta_w\approx\frac{\theta_P\,\Delta\xi_W+\theta_W\,\Delta\xi_P}{\Delta\xi_P+\Delta\xi_W} \tag{21}$$

UDS approximation for advection term:

$$\frac{(\theta_e-\theta_w)}{\Delta\xi_P}\approx\frac{U_P\,(\theta_P-\theta_W)}{\frac{\Delta\xi_W+\Delta\xi_P}{2}} \tag{22}$$

3.1 Discretized equations

UDS discretization:

- channel entrance (volumes adjacent to $\xi=0$):

$$\mathrm{Fo}^{-1}\frac{\mathrm{d}\theta_P}{\mathrm{d}\tau}+\frac{1}{2}U_P\,\frac{\theta_P-\theta_w}{\Delta\xi_P/2}=\frac{\theta_N-2\,\theta_P+\theta_S}{\Delta\eta^2} \tag{23}$$

- channel centerline (volumes adjacent to $\eta=0$):

$$\mathrm{Fo}^{-1}\frac{\mathrm{d}\theta_P}{\mathrm{d}\tau}+\frac{1}{2}U_P\,\frac{\theta_P-\theta_W}{(\Delta\xi_P+\Delta\xi_W)/2}=\frac{\theta_N-\theta_P}{\Delta\eta^2} \tag{24}$$

- channel wall (volumes adjacent to $\eta=1$):

$$\mathrm{Fo}^{-1}\frac{\mathrm{d}\theta_P}{\mathrm{d}\tau}+\frac{1}{2}U_P\,\frac{\theta_P-\theta_W}{(\Delta\xi_P+\Delta\xi_W)/2}=\left(\frac{\partial\theta}{\partial\eta}\right)_n-\frac{\theta_P-\theta_S}{\Delta\eta^2} \tag{25}$$

$$\left(\frac{\partial\theta}{\partial\eta}\right)_n=-(R^*\,\mathrm{Fo}_s)^{-1}\frac{\mathrm{d}\theta_n}{\mathrm{d}\tau},\qquad\theta_n=(3\,\theta_P-\theta_S)/2 \tag{26}$$

resulting in:

$$\left(\mathrm{Fo}^{-1}+\frac{3}{2}\,(R^*\,\mathrm{Fo}_s)^{-1}\right)\frac{\mathrm{d}\theta_P}{\mathrm{d}\tau}-\frac{1}{2}\,(R^*\,\mathrm{Fo}_s)^{-1}\frac{\mathrm{d}\theta_S}{\mathrm{d}\tau}+ \\ +\frac{1}{2}U_P\,\frac{\theta_P-\theta_W}{(\Delta\xi_P+\Delta\xi_W)/2}=-\frac{\theta_P-\theta_S}{\Delta\eta^2} \tag{27}$$

- volume adjacent to the corner at $\eta = 0$ and $\xi = 0$:

$$\mathrm{Fo}^{-1}\,\frac{\mathrm{d}\theta_P}{\mathrm{d}\tau} + \frac{1}{2}\,U_P\,\frac{\theta_P - \theta_w}{\Delta\xi_P/2} = \frac{\theta_N - \theta_P}{\Delta\eta^2} \tag{28}$$

- volume adjacent to the corner at $\eta = 1$ and $\xi = 0$:

$$\left(\mathrm{Fo}^{-1} + \frac{3}{2}\,(R^*\,\mathrm{Fo}_s)^{-1}\right)\frac{\mathrm{d}\theta_P}{\mathrm{d}\tau} - \frac{1}{2}\,(R^*\,\mathrm{Fo}_s)^{-1}\,\frac{\mathrm{d}\theta_S}{\mathrm{d}\tau} + \\ + \frac{1}{2}\,U_P\,\frac{\theta_P - \theta_w}{\Delta\xi_P/2} = -\frac{\theta_P - \theta_S}{\Delta\eta^2} \tag{29}$$

- inner volumes:

$$\mathrm{Fo}^{-1}\,\frac{\mathrm{d}\theta_P}{\mathrm{d}\tau} + \frac{1}{2}\,U_P\,\frac{\theta_P - \theta_W}{(\Delta\xi_P + \Delta\xi_W)/2} = \frac{\theta_N - 2\,\theta_P + \theta_S}{\Delta\eta^2} \tag{30}$$

After rearranging one arrives at:

- channel entrance (volumes adjacent to $\xi = 0$):

$$\frac{\mathrm{d}\theta_P}{\mathrm{d}\tau} = \mathrm{Fo}\left(-\frac{1}{2}\,U_P\,\frac{\theta_P - \theta_w}{\Delta\xi_P/2} + \frac{\theta_N - 2\,\theta_P + \theta_S}{\Delta\eta^2}\right) \tag{31}$$

- channel wall (volumes adjacent to $\eta = 1$):

$$\left(1 + \frac{3}{2}\,\frac{\mathrm{Fo}}{R^*\,\mathrm{Fo}_s}\right)\frac{\mathrm{d}\theta_P}{\mathrm{d}\tau} - \frac{1}{2}\,\frac{\mathrm{Fo}}{R^*\,\mathrm{Fo}_s}\,\frac{\mathrm{d}\theta_S}{\mathrm{d}\tau} = \mathrm{Fo}\left(-\frac{1}{2}\,U_P\,\frac{\theta_P - \theta_W}{(\Delta\xi_P + \Delta\xi_W)/2} - \frac{\theta_P - \theta_S}{\Delta\eta^2}\right) \tag{32}$$

$$\frac{\mathrm{d}\theta_S}{\mathrm{d}\tau} = \mathrm{Fo}\left(-\frac{1}{2}\,U_S\,\frac{\theta_S - \theta_{SW}}{(\Delta\xi_P + \Delta\xi_W)/2} + \frac{\theta_P - 2\,\theta_S + \theta_{SS}}{\Delta\eta^2}\right) \tag{33}$$

- channel centerline (volumes adjacent to $\eta = 0$):

$$\frac{\mathrm{d}\theta_P}{\mathrm{d}\tau} = \mathrm{Fo}\left(-\frac{1}{2}\,U_P\,\frac{\theta_P - \theta_W}{(\Delta\xi_P + \Delta\xi_W)/2} + \frac{\theta_N - \theta_P}{\Delta\eta^2}\right) \tag{34}$$

- volume adjacent to the corner at $\eta = 0$ and $\xi = 0$:

$$\frac{\mathrm{d}\theta_P}{\mathrm{d}\tau} = \mathrm{Fo}\left(-\frac{1}{2}\,U_P\,\frac{\theta_P - \theta_w}{\Delta\xi_P/2} + \frac{\theta_N - \theta_P}{\Delta\eta^2}\right) \tag{35}$$

- volume adjacent to the corner at $\eta = 1$ and $\xi = 0$:

$$\left(1 + \frac{3}{2}\,\frac{\mathrm{Fo}}{R^*\,\mathrm{Fo}_s}\right)\frac{\mathrm{d}\theta_P}{\mathrm{d}\tau} - \frac{1}{2}\,\frac{\mathrm{Fo}}{R^*\,\mathrm{Fo}_s}\,\frac{\mathrm{d}\theta_S}{\mathrm{d}\tau} = \mathrm{Fo}\left(-\frac{1}{2}\,U_P\,\frac{\theta_P - \theta_w}{\Delta\xi_P/2} - \frac{\theta_P - \theta_S}{\Delta\eta^2}\right) \tag{36}$$

$$\frac{\mathrm{d}\theta_S}{\mathrm{d}\tau} = \mathrm{Fo}\left(-\frac{1}{2}\,U_S\,\frac{\theta_S - \theta_{Sw}}{\Delta\xi_P/2} + \frac{\theta_P - 2\,\theta_S + \theta_{SS}}{\Delta\eta^2}\right) \tag{37}$$

- for remaining volumes:

$$\frac{\mathrm{d}\theta_P}{\mathrm{d}\tau} = \mathrm{Fo}\left(-\frac{1}{2}\,U_P\,\frac{\theta_P - \theta_W}{(\Delta\xi_P + \Delta\xi_W)/2} + \frac{\theta_N - 2\,\theta_P + \theta_S}{\Delta\eta^2}\right) \tag{38}$$

3.2 ODE system

Computational cell numbering:

$$k = (j-1)\, I + i \tag{39}$$

$$P = k, \qquad E = k+1, \qquad W = k-1, \qquad N = k+I, \qquad S = k-I, \tag{40}$$

$$SS = k - 2\,I, \qquad SW = k - 1 - I, \qquad SE = k + 1 - I, \tag{41}$$

Generalized ODE system:

$$\frac{\mathrm{d}\theta_k}{\mathrm{d}\tau} = F_k(\theta_1, \ldots, \theta_K, \tau) \tag{42}$$

Discretization functions:

- for $k = 1$:

$$F_k = \mathrm{Fo}\left(-\frac{1}{2}\, U_P \,\frac{\theta_P - \theta_w}{\Delta\xi_P/2} + \frac{\theta_N - \theta_P}{\Delta\eta^2} \right) \tag{43}$$

- for $1 < k \leq I$:

$$F_k = \mathrm{Fo}\left(-\frac{1}{2}\, U_P \,\frac{\theta_P - \theta_W}{(\Delta\xi_P + \Delta\xi_W)/2} + \frac{\theta_N - \theta_P}{\Delta\eta^2} \right) \tag{44}$$

- for $I + 1 \leq k \leq I\,(J-2) + 1$ and $\mod(k, I) = 1$:

$$F_k = \mathrm{Fo}\left(-\frac{1}{2}\, U_P \,\frac{\theta_P - \theta_w}{\Delta\xi_P/2} + \frac{\theta_N - 2\,\theta_P + \theta_S}{\Delta\eta^2} \right) \tag{45}$$

- for $k = I\,(J-1) + 1$:

$$\begin{aligned} F_k = \mathrm{Fo}\left(1 + \frac{3}{2}\,\frac{\mathrm{Fo}}{R^*\,\mathrm{Fo}_s}\right)^{-1} &\left[\left(-\frac{1}{2}\, U_P \,\frac{\theta_P - \theta_w}{\Delta\xi_P/2} - \frac{\theta_P - \theta_S}{\Delta\eta^2} \right) + \right. \\ &\left. + \frac{1}{2}\,\frac{\mathrm{Fo}}{R^*\,\mathrm{Fo}_s} \left(-\frac{1}{2}\, U_S \,\frac{\theta_S - \theta_{Sw}}{\Delta\xi_P/2} + \frac{\theta_P - 2\,\theta_S + \theta_{SS}}{\Delta\eta^2} \right) \right] \end{aligned} \tag{46}$$

- for $I\,(J-1) + 1 < k \leq I\,J$:

$$\begin{aligned} F_k = \mathrm{Fo}\left(1 + \frac{3}{2}\,\frac{\mathrm{Fo}}{R^*\,\mathrm{Fo}_s}\right)^{-1} &\left[\left(-\frac{1}{2}\, U_P \,\frac{\theta_P - \theta_W}{(\Delta\xi_P + \Delta\xi_W)/2} - \frac{\theta_P - \theta_S}{\Delta\eta^2} \right) + \right. \\ &\left. + \frac{1}{2}\,\frac{\mathrm{Fo}}{R^*\,\mathrm{Fo}_s} \left(-\frac{1}{2}\, U_S \,\frac{\theta_S - \theta_{SW}}{(\Delta\xi_P + \Delta\xi_W)/2} + \frac{\theta_P - 2\,\theta_S + \theta_{SS}}{\Delta\eta^2} \right) \right] \end{aligned} \tag{47}$$

- for remaining nodes:

$$F_k = \mathrm{Fo}\left(-\frac{1}{2}\, U_P \,\frac{\theta_P - \theta_W}{(\Delta\xi_P + \Delta\xi_W)/2} + \frac{\theta_N - 2\,\theta_P + \theta_S}{\Delta\eta^2} \right) \tag{48}$$

Naturally:

$$\theta_w = \theta_{Sw} = \theta_{in} \tag{49}$$

4. RESULTS AND DISCUSSION

4.1 Validation

Before going into the presentation of general simulation results, a convergence analysis and comparisons with previous published results are performed for validation purposes. The next tables, present convergence results for a case with large fluid Fourier number and a negligible wall Fourier number. This configuration corresponds to uniform wall temperature condition (since the storage effect in the matrix is reduced to a negligible value). In addition, the large fluid Fourier value leads to a solution that is already in steady-state. Hence, literature results are used for validation, obtained from (Chalhub et al., 2008) , so the result for steady state and uniform temperature on the wall is exactly equal with five decimal places. These tables presents convergence results for different grid spacing, given by a spacing function defined as $f(\xi) = \xi^a$, with $a = 1$ corresponding to a uniform grid. Tables 1, 2 and 3 present the convergence results for $a = 1$, 2, and 3. As can be seen as the grid is refined in both directions, the solution progressively converges to the literature results, thereby validating the proposed solution scheme. However, it is interesting to note that for uniform grids, the solution near the channel entrance possess a very poor convergence behavior, due to the large temperature gradients that can occur in this region. This effect is significant minimized when a non uniform gird (with grid points concentrated near the entrance) is used, as seen for the cases with $a = 2$ and $a = 3$.

Table 1. Nusselt number with $R^*\mathrm{Fo}_s = 10^{-10}$, $\tau = 1$, $\mathrm{Fo} = 10$ and mesh with $a = 1$.

$R^*\mathrm{Fo}_s$	a	I	J	$\xi = 0.001$	$\xi = 0.01$	$\xi = 0.1$	$\xi = 1$
10^{-10}	1	12	12	94.3015	78.6727	9.16472	7.53167
10^{-10}	1	12	25	196.2380	161.5270	9.29596	7.53960
10^{-10}	1	12	50	392.3180	320.8170	9.32846	7.54055
10^{-10}	1	12	100	784.6110	639.4680	9.33703	7.54073
10^{-10}	1	12	200	1569.0000	1276.6300	9.33914	7.54070
10^{-10}	1	25	12	92.3201	57.0013	8.05481	7.53167
10^{-10}	1	25	25	191.6910	112.5100	8.06740	7.53961
10^{-10}	1	25	50	382.8110	218.8710	8.06835	7.54055
10^{-10}	1	25	100	765.1290	431.5090	8.06834	7.54073
10^{-10}	1	25	200	1529.6600	856.7200	8.06833	7.54070
10^{-10}	1	50	12	88.5075	14.8521	7.83967	7.53167
10^{-10}	1	50	25	182.8660	15.8853	7.84814	7.53961
10^{-10}	1	50	50	364.2390	16.1799	7.84867	7.54055
10^{-10}	1	50	100	726.9700	16.2621	7.84863	7.54073
10^{-10}	1	50	200	1452.4500	16.2838	7.84861	7.54070
10^{-10}	1	100	12	80.9935	14.8521	7.72134	7.53167
10^{-10}	1	100	25	165.2910	15.8853	7.72833	7.53961
10^{-10}	1	100	50	326.9170	16.1799	7.72874	7.54055
10^{-10}	1	100	100	650.0230	16.2621	7.72876	7.54073
10^{-10}	1	100	200	1296.2000	16.2838	7.72868	7.54070
10^{-10}	1	200	12	66.4168	13.2945	7.67041	7.53167
10^{-10}	1	200	25	130.742	13.6141	7.67695	7.53961
10^{-10}	1	200	50	252.583	13.6585	7.67734	7.54055
10^{-10}	1	200	100	495.628	13.6643	7.67736	7.54073
10^{-10}	1	200	200	981.528	13.665	7.67729	7.54070
steady state, uniform wall temperature				24.6882	12.0145	7.63215	7.54070

After presenting the previous convergence analysis, simulation results are carried-out for investigating the effects of energy storage in the matrix and the transient solution on the Nusselt number. Table 4 presents the calculated values for the Nusselt number on different axial positions for $\mathrm{Fo} = 10$ and different values of product $R^*\mathrm{Fo}_s$. As can be seen as $R^*\mathrm{Fo}_s$ is increased, the Nusselt number gradually diminishes tending to negligible value. This occurs because the product $R^*\mathrm{Fo}_s$ is inversely proportional to the heat capacity of the channel wall. As the wall heat capacity is decreased is reaches thermal equilibrium faster with the fluid, leading situation where heat transfer process ceases.

Next, in table 5, similar results are presented. Similar considerations regarding the results can be made to this situation. The main difference is that for this case the lower fluid Fourier number corresponds to a situation closer to the initial conditions (farther away from the steady-state solution). As a result, the decrease in the Nusselt number with increasing $R^*\mathrm{Fo}_s$ is less pronouced.

Table 2. Nusselt number with $R^*\mathrm{Fo}_s = 10^{-10}$, $\tau = 1$, $\mathrm{Fo} = 10$ and mesh with $a = 2$.

$R^*\mathrm{Fo}_s$	a	I	J	$\xi = 0.001$	$\xi = 0.01$	$\xi = 0.1$	$\xi = 1$
10^{-10}	2	12	12	74.5179	15.7839	8.05633	7.41071
10^{-10}	2	12	25	149.995	17.2014	8.06845	7.48126
10^{-10}	2	12	50	294.141	17.6284	8.06933	7.51126
10^{-10}	2	12	100	582.106	17.7506	8.06931	7.54068
10^{-10}	2	12	200	1157.94	17.7833	8.0693	7.54064
10^{-10}	2	25	12	24.7618	13.2548	7.80626	7.48004
10^{-10}	2	25	25	31.374	13.5548	7.81418	7.51484
10^{-10}	2	25	50	33.8872	13.5953	7.81466	7.52816
10^{-10}	2	25	100	34.6899	13.6005	7.81467	7.54073
10^{-10}	2	25	200	34.916	13.6011	7.81459	7.54069
10^{-10}	2	50	12	23.7957	12.6541	7.70565	7.50704
10^{-10}	2	50	25	27.9475	12.8443	7.71247	7.52782
10^{-10}	2	50	50	28.8277	12.8668	7.71287	7.53466
10^{-10}	2	50	100	28.9754	12.8694	7.71289	7.54073
10^{-10}	2	50	200	28.9961	12.8696	7.71281	7.5407
10^{-10}	2	100	12	23.5083	12.2429	7.66276	7.51963
10^{-10}	2	100	25	27.0317	12.3872	7.66925	7.53385
10^{-10}	2	100	50	27.6802	12.4034	7.66964	7.53767
10^{-10}	2	100	100	27.779	12.4051	7.66966	7.54073
10^{-10}	2	100	200	27.792	12.4053	7.66959	7.5407
10^{-10}	2	200	12	22.9688	12.0576	7.64369	7.52571
10^{-10}	2	200	25	25.5247	12.185	7.65006	7.53677
10^{-10}	2	200	50	25.9329	12.199	7.65046	7.53913
10^{-10}	2	200	100	25.9901	12.2005	7.65048	7.54073
10^{-10}	2	200	200	25.9973	12.2006	7.65041	7.54070
steady state, uniform wall temperature				24.6882	12.0145	7.63215	7.54070

5. CONCLUSIONS

This study presented a formulation for investigating the effect of transient heat transfer in laminar duct flow, having applications in regenerative heat exchange. The objective of the study was to analyze the variation of the convective heat transfer coefficient in transient heat transfer with energy storage in the duct wall, in order to simulate conditions found in regenerative heat exchangers. This was motivated because of the fact that most formulations used for analyzing and thermal designing heat regenerators are based on constant heat transfer coefficient. The presented formulation was normalized using traditional dimensionless groups in convective heat transfer, and a numerical solution based on the Finite Volumes Method combined with the Numerical Method of Lines was implemented in the Mathematica system. The implementation was validated against previous literature results. Then, simulation results were conducted to illustrate the effect of varying wall heat capacity and fluid Fourier number. The results indicate that there is a great variation on the Nusselt number, especially when a transient regime is in effect and/or wall storage effects are considered. Finally, one should mention that these results are still preliminary and there is considerable need for future research.

6. ACKNOWLEGEMENTS

The authors would like to acknowledge the financial support provided by FAPERJ, CAPES, CNPq and Universidade Federal Fluminense.

Table 3. Nusselt number with $R^{*}\mathrm{Fo}_s = 10^{-10}$, $\tau = 1$, $\mathrm{Fo} = 10$ and mesh with $a = 3$.

$R^{*}\mathrm{Fo}_s$	a	I	J	$\xi = 0.001$	$\xi = 0.01$	$\xi = 0.1$	$\xi = 1$
10^{-10}	3	12	12	25.914	13.4743	7.95746	7.30117
10^{-10}	3	12	25	35.401	13.8117	7.96763	7.4273
10^{-10}	3	12	50	39.7125	13.858	7.96831	7.48378
10^{-10}	3	12	100	41.2165	13.864	7.96828	7.54022
10^{-10}	3	12	200	41.6594	13.8647	7.96826	7.54016
10^{-10}	3	25	12	23.9272	12.8217	7.77613	7.44601
10^{-10}	3	25	25	28.5335	13.0353	7.78366	7.49841
10^{-10}	3	25	50	29.644	13.0613	7.7841	7.51991
10^{-10}	3	25	100	29.846	13.0643	7.78411	7.54073
10^{-10}	3	25	200	29.8758	13.0646	7.78403	7.54069
10^{-10}	3	50	12	23.393	12.3303	7.69848	7.49291
10^{-10}	3	50	25	26.608	12.4828	7.70523	7.52104
10^{-10}	3	50	50	27.1609	12.5001	7.70562	7.53126
10^{-10}	3	50	100	27.2421	12.5019	7.70564	7.54073
10^{-10}	3	50	200	27.2525	12.5021	7.70556	7.54069
10^{-10}	3	100	12	22.9161	12.093	7.6594	7.51318
10^{-10}	3	100	25	25.3787	12.2233	7.66587	7.53076
10^{-10}	3	100	50	25.7674	12.2377	7.66626	7.53613
10^{-10}	3	100	100	25.8214	12.2392	7.66628	7.54073
10^{-10}	3	100	200	25.8282	12.2394	7.66621	7.5407
10^{-10}	3	200	12	22.6771	11.9923	7.64218	7.52263
10^{-10}	3	200	25	24.8377	12.1142	7.64854	7.53529
10^{-10}	3	200	50	25.1702	12.1275	7.64894	7.53839
10^{-10}	3	200	100	25.2155	12.1289	7.64897	7.54073
10^{-10}	3	200	200	25.2211	12.1290	7.64890	7.54070
steady state, uniform wall temperature				24.6882	12.0145	7.63215	7.54070

Table 4. Nusselt values for $\mathrm{Fo} = 10$.

$R^{*}\mathrm{Fo}_s$	$\xi = 0.001$	$\xi = 0.01$	$\xi = 0.1$	$\xi = 1$
10^{-10}	25.0472	12.1127	7.64890	7.54070
10^{-4}	23.0250	11.6039	7.40000	7.33096
10^{-3}	7.73277	7.42914	5.60789	6.13104
10^{-2}	0.00000	0.00248	0.327955	2.46409

Table 5. Nusselt values for $\mathrm{Fo} = 1$.

$R^{*}\mathrm{Fo}_s$	$\xi = 0.001$	$\xi = 0.01$	$\xi = 0.1$	$\xi = 1$
10^{-10}	25.4485	12.2108	7.72876	3.23164
10^{-4}	24.3169	11.9424	7.61191	3.22696
10^{-3}	15.0291	9.68616	6.67298	3.18525
10^{-2}	0.00343	0.564202	2.31506	2.82355

7. REFERENCES

Chalhub, D.J.N.M., Dias, R.A.C., Machado, F.J.F., and Sphaier, L.A., 2008, "Comparisons between GITT and FVM solutions for thermally developing flow in parallel-plates channels", in "Proceedings of the 12th Brazilian Congress of Thermal Sciences and Engineering (ENCIT)", Belo Horizonte, MG.

de Monte, F., 1999, "Cyclic steady thermal response of rapidly switchedfixed-bed heat regenerators in counterflow", International Journal of Heat and Mass Transfer, vol. 42, no. 14, pp. 2591–2604.

Holmberg, R.B., 1977, "Heat and mass transfer in rotary heat exchangers with nonhygroscopic rotor materials", Journal of Heat Transfer (ASME), vol. 99, pp. 196–202.

Nogueira, D. and Sphaier, L.A., 2008, "Análise da utilização de coeficientes convectivos variáveis na transferência de calor e massa em regeneradores rotativos", in "Anais do V Congresso Nacional de Engenharia Mecânica – CONEM", Salvador, BA, Brazil.

Nogueira, D. and Sphaier, L.A., 2009, "Solution strategies for thermally developing channel flow using finite volumes and the method of lines", in "Anais XII Encontro de Modelagem Computacional", Rio de Janeiro, RJ.

Saastamoinen, J.J., 1999, "Heat transfer in crossflow regenerators", International Journal of Heat and Mass Transfer, vol. 42, no. 17, pp. 3205–3216.

Shen, C.M. and Worek, W.M., 1992, "The effect of wall conduction on the performance of regenerative heat exchangers", Energy, vol. 17, no. 12, pp. 1199–1213.

Shen, C.M. and Worek, W.M., 1993a, "A correlation for the heat conduction effect in counterflow rotary regenerative heat exchangers", Journal of Energy Resources Technology (ASME), vol. 115, pp. 287–290.

Shen, C.M. and Worek, W.M., 1993b, "Second-law optimization of regenerative heat exchangers, including the effect of matrix heat conduction", Energy, vol. 18, no. 4, pp. 355–363.

Sphaier, L.A. and Worek, W.M., 2004, "Analysis of heat and mass transfer in porous sorbents used in rotary regenerators", International Journal of Heat and Mass Transfer, vol. 47, no. 14-16, pp. 3415–3430.

Sphaier, L.A. and Worek, W.M., 2009, "Parametric analysis of heat and mass transfer regenerators using a generalized effectiveness-NTU method", International Journal of Heat and Mass Transfer, vol. 52, pp. 2265–2272.

8. RESPONSIBILITY NOTICE

The authors are the only responsible for the printed material included in this paper.